Geology-based Shear Wave Velocity Profile Modelling for Ground Motion Simulation

Yuxiang Tang[1], Nelson Lam[1], Hing-Ho Tsang[2], Elisa Lumantarna[1],

1. Corresponding Author, Department of Infrastructure Engineering, The University of Melbourne, Parkville, VIC 3010, Australia. Email: yuxiangt@student.unimelb.edu.au

   Professor, Department of Infrastructure Engineering, The University of Melbourne, Parkville, VIC 3010, Australia. Email: ntkl@unimelb.edu.au

   Lecturer, Department of Infrastructure Engineering, The University of Melbourne, Parkville, VIC 3010, Australia. Email: elu@unimelb.edu.au

2. Senior Lecturer, Department of Civil and Construction Engineering, Swinburne University of Technology, Melbourne, VIC 3122, Australia. Email: htsang@swin.edu.au

1. Introduction

Seismic hazard analysis for the regions of low-to-moderate seismicity can be very challenging for the acute scarcity of strong motion data on rock site in these regions, such as Australia continent, Singapore, and South-eastern China. A realistic modelling approach for seismic hazard assessment purpose in stable continental regions (SCRs) and other intraplate regions can be achieved by combining the earthquake source model, path model, and crustal model through stochastic simulations (Boore and Joyner 1997, Lam, et al. 2000a, Boore 2003a, Chandler, et al. 2006b). The regional path model and local crustal model are of fundamental significance for modelling the ground motions for such regions with possibly low uncertainties and variabilities (Lam, et al. 2000b, Atkinson and Boore 2006). For local crustal model, often two effects are considered: crustal amplification effect of the seismic waves when they cross the boundary between different mediums, and the crustal attenuation effect which is associated with the transmission quality of the crustal layers, and the two effects are recently observed from the instrumental records from deep drill-holes in active seismic areas (Abercrombie 1997).

Shear Wave Velocity (SWV) profiles are essentially required to model the crustal amplification effect. Quarter-wavelength approximation (QWA) or so called Square root impedance (SRI) method (Joyner, et al. 1981, Boore and Joyner 1997) is often used to compute the frequency-dependent crustal amplification factor. To use this method, local SWV velocity and density profiles are required in the first place.

Seismic wave velocity (including compressional velocity and shear-wave velocity) model is often obtained from refraction and reflection surveys. However, the seismic wave velocity structures obtained by the approaches above are not convenient for use for seismic hazard purpose because no parameterized functional form is given, and seismic wave profile modelling still requires more attention.

Boore and Joyner (1997) (abbreviated as **BJ97** model in the following context) constructed a model for seismic shear-wave velocity as a function of depth for generic rock (GR) site and generic very hard rock (GHR) site, based on borehole data and studies of crustal velocities. Boore (2016) put forward a slowness (reciprocal of SWV) interpolation method to construct the SWV profile with specific V_{S30} (time-averaged SWV at upper 30 m) values using the profile of GR site and GHR site. The advantage of **BJ97** model to construct SWV profile is that it's quite simple and straightforward. However, the accuracy of the profile is not convincing as no local geological information is considered in the model.

Chandler, et al. (2005) (abbreviated as **CLT05** model in the following context) proposed a geology-based SWV profile modelling approach based on *P*-wave (compressional wave) and V_S/V_P ratio. Moreover, the global crust model CRUST2.0 is adopted to gather the geological information for different regions to verify the proposed SWV profile model. **CLT05** model has been proved to be capable of predicting SWV profile for various conditions with reasonable accuracy. However, after prudent investigation, the V_S/V_P ratio adopted in **CLT05** model is conservative compared to other studies, and thus the proposed V_S profile is conservative, especially for shallow depth (< 4 km). Additionally, CRUST2.0 (with a 2° × 2° resolution) database (which was used to obtain the geological information for constructing **CLT05**) (https://igppweb.ucsd.edu/~gabi/crust2.html) has been abolished by scholars as CRUST1.0

(with a 1° × 1° resolution) database (https://igppweb.ucsd.edu/~gabi/crust1.html) has been adopted instead nowadays. The introduction of CRUST1.0 can be found in section 2. Thus, a new updated SWV modelling approach is acutely needed for seismic hazard assessment purpose.

Most existing Ground Motion Prediction Equations (GMPEs) nowadays are developed based on the general broad geographical sub-division of a region, such as, Middle East (Ambraseys, et al. 2005), Eastern North America (Atkinson and Boore 1995, Atkinson 2004, Atkinson and Boore 2006, Atkinson 2008, Atkinson and Boore 2014, Yenier and Atkinson 2015), Western Australia (Allen, et al. 2006, Liang, et al. 2008), South-eastern Australia (Allen 2012). When these GMPEs are taken as the input for *Probabilistic Seismic Hazard Analysis* (PSHA), the results may differ by more than 100% even for same earthquake scenarios, tectonic classifications, and return periods (Lam, et al. 2016). The inter-regional uncertainty in the bedrock conditions is obvious. Moreover, if various geological site conditions have been reported within a region (e.g. south-eastern China), the enlisted GMPEs would not give relatively accurate estimates for the local variability (intra-regional uncertainty). Thus, a much more comprehensive modelling methodology is required to cope with the local geological conditions of both surface sediments and bedrock to remove the inter-regional and intra-regional uncertainty.

The purpose of this paper is to propose a more comprehensive SWV profiling model, which can be used to construct the SWV profile for any region in SCR or other low-to-moderate seismicity regions for seismic hazard assessment purpose, based on the available information which can be obtained from CRUST1.0 and existing field recordings. A brief introduction of CRUST1.0 database is given in section 2. The well-known tri-linear *P*-wave model is introduced in section 3.1. A newly developed V_S/V_P model as a function of depth using data from various sources is put forward in section 3.2, and six frequently encountered cases with the corresponding V_S models are given in section 3.3. Seven case studies from typical low-to-moderate seismicity regions are adopted in section 4 to validate the proposed SWV profiling model.

This paper only concerns the SWV profiling model on rock sites, the site response on soil sedimentary is beyond the scope of this paper. The application of the proposed SWV profiling model will be discussed in other papers due to the length limitation.

CRUST1.0 (https://igppweb.ucsd.edu/~gabi/crust1.html) is a global crustal model at 1° × 1°, an update of CRUST5.1 and CRUST2.0 (https://igppweb.ucsd.edu/~gabi/crust2.html). The new model incorporates an updated version of global sediment thickness. The principle crustal types of the new model are adopted from CRUST5.1, and the additional crustal types mark specific tectonic settings, such as continental rifts, continental shelves and oceanic plateaus. In contrast to older models, the function of crustal types in the new model is limited to assigning elastic parameters to layers in the crystalline crust. CRUST1.0 consists of less than 40 crustal types, each of the 1° × 1° cells have a unique 8-layer crustal profile where the layers are: 1) water; 2) ice; 3) upper sediments; 4) middle sediments; 5) lower sediments; 6) crystalline upper crust; 7) crystalline middle crust; 8) crystalline lower crust. Parameters like compressional wave velocity (V_P), shear wave velocity (V_S) and crust density (ρ) are given explicitly for each layer. The updated relationships between Poisson's ratio and shear-wave velocity, compressional wave velocity and shear-wave velocity, crustal density and shear-wave velocity,

are all adopted from Brocher's study which published in 2005 (Brocher 2005), as the study used comprehensive dataset and obtained reasonably accuracy. More introduction of global crustal models can be found from the paper published by Chandler, et al. (2005).

2. Shear-wave velocity modelling

This section introduces the detailed modelling process of near source shear-wave velocity profile for rock crust, which can be used for seismic hazard analysis. As mentioned above, according to the conclusion obtained by Brocher (2005), the estimates of compressional wave velocity (V_P) are reasonably accurate in most cases. However, the estimates of shear-wave velocity (V_S) are not accurate in most cases (Brocher, et al. 1997a, Fletcher, et al. 2003). The reason is that the relationship between V_P and V_S are always inappropriate. Thus, in this study, compressional wave velocity profile modelling from previous studies would be adopted in the first place (section 3.1). Then detailed tri-linear form V_S/V_P would be modelled based on recording data and existing studies (section 3.2). The updated *Vs* profile model for rock crust would then be proposed combining V_P profile model and V_S/V_P model (section 3.3).

2.1 Compressional (P) wave velocity profile modelling

The previous studies show that compressional wave is closely related to crustal structure, depth, temperature, geological age of rock formation, and even chemical compositions of the sediments (Faust 1951, Downs 1993, Christensen 1995, Magistrale, et al. 1996). For seismic rick analysis purpose, the modern 3-D compressional wave velocity profiles obtained from seismic refraction and reflection surveys are not convenient for use in engineering seismology, as they do not provide any specific mathematic expressions (Fliedner, et al. 2000, Qiu, et al. 2010, Zhao, et al. 2013, Lee, et al. 2015). In this study, the non-linear form first proposed by Faust (1951) and further developed by Chandler, et al (2006) is adopted. This geology-based velocity model (GBVM) had been proved to be valid for kinds of rock sites. The tri-liner form of this model is summarized as equation (1):

$$V_P = V_{P0.03} \left(\frac{Z}{0.03}\right)^{1/6} \quad Z \le Z_S \tag{1a}$$

$$V_P = V_{PZc} \left(\frac{Z}{Zc}\right)^{n} \quad Z_S < Z \le Z_C \tag{1b}$$

$$n = \frac{\log(V_{PZc}/V_{PZs})}{\log(Zc/Zs)} \tag{1c}$$

$$V_P = V_{P8} \left(\frac{Z}{8}\right)^{1/12} \quad Z > Z_C \tag{1d}$$

where, $V_{P0.03}$, V_{PZc}, V_{P8} are the reference V_P value at depth of 0.03 km, Z_C km, and 8 km respectively; and Z_S, Z_C are the depth of upper sedimentary crustal layer and the combined soft and hard sedimentary crustal rock layers (Chandler, et al. 2005). The whole function can also be illustrated by Figure 1.

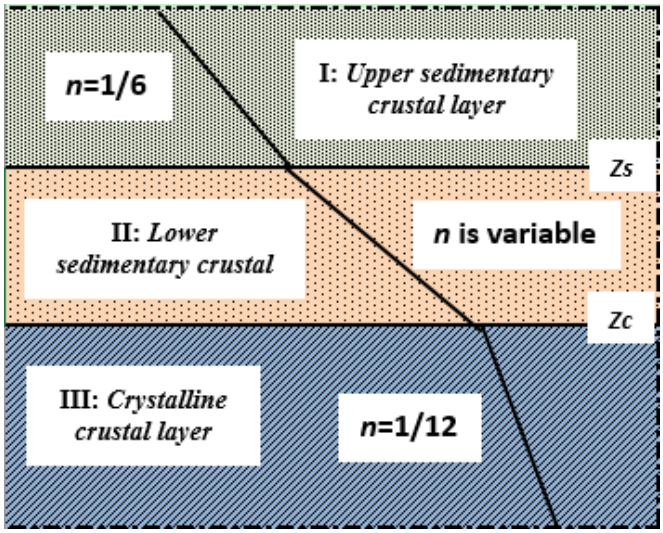

Figure 1. Illustration of V_P profile modelling. Three sedimentary crustal layers are defined. Z_S and Z_C are defined as the thickness of upper sedimentary crustal layer and total sedimentary crustal layer respectively. n is the exponent in the non-linear functional form for constructing V_P profile

The detailed modelling process and the validation of this tri-linear functional form can be found in Chandler, et al. (2005).

2.2 Modelling of V_S/V_P

The V_S-V_P relationship is quite important for the analysis of reservoir geo-mechanical properties for studying seismic ground motions. However, SWV records are often not available due to technological limitations, especially for large depth. Alternatively, we can obtain SWV from empirical prediction equations based on the records of compressional wave velocity (V_P). In **BJ97** (Boore and Joyner 1997) model, Boore and Joyner obtained the SWV profiles from two generic approach: one is the SWV data from boreholes in upper 4 km; another one is the data of compressional wave velocity profile together with the V_S-V_P relationship ($V_S/V_P=1/\sqrt{3}$) for the depth below 4 km. For this study, the SWV profiles will be derived from compressional wave velocity completely. Thus, the V_S-V_P relationship is of extremely importance to obtain a reasonably accurate SWV profiles. To obtain a more reasonable V_S-V_P relationship, the recording data from multiple sources all around world are summarized in Table 1, and a thorough regression analysis for the ratio (V_S/V_P) will be conducted using this dataset.

Table 1. Field measurement data used for regression analysis

Region	Number of recordings	Citations
ENA, WNA, E-China	81	Laske, et al. (2000)
Hong Kong	5	Tam (2002)
San Andreas, Central California	3	Malin, et al. (1981)
Michigan Basin	20	Stewart, et al. (1981)
Imperial Valley, Southern California	3	Archuleta (1982)
Eastern Sierra Nevada	7	Fliedner and Klemperer (2000)
South-central Alaska	7	Brocher, et al. (2004)
Lithologies sampled in 30m-deep boreholes	96	Boore (2003b)
San Francisco Bay Area	6	Baise, et al. (2003)
Kilauea caldera	3	Lin, et al. (2015)
Oceanic crust-uppermost mantle condition	6	Saito, et al. (2015)
Indian subcontinent	11	Bhowmick (2017)

After trials and errors, a tri-linear functional form is adopted, as it can achieve more accurate predictions with smallest residuals. During the regression analysis, the power functional form is found to be more powerful than any other functional forms, including polynomial and exponential form. What's more, two intercept points (0.2 km and 2.0 km) are found which have never been found in any previous studies. For depth smaller than 0.2 km, the gradient of V_S/V_P is quite large, and the gradient of V_S/V_P between 0.2 and 2.0 km will become much smaller, for depth greater than 2.0 km, the value of V_S/V_P is almost keeping constant. From the study of Brocher (2005), V_S/V_P is closely related to Poisson's ratio, and functional form obtained by Brocher is expressed in equation 2:

$$\sigma = 0.5\frac{(VS/VP)^2-2}{(VS/VP)^2-1} \quad (2)$$

where σ is Poisson's ratio.

For crustal rock sites, σ is frequently assumed to 0.25 (and thus $V_S/V_P = 0.577$), which is also corresponding to the results obtained by Chandler, et al. (2005). Therefore, in this study, the constant value of V_S/V_P for the depth greater than 2.0 km is fixed at 0.577. The corresponding V_S/V_P zones are defined as A, B, C respectively based on different V_S/V_P functional forms.

The result can be found in **Figure 2**. The specific function is expressed in equation 3.

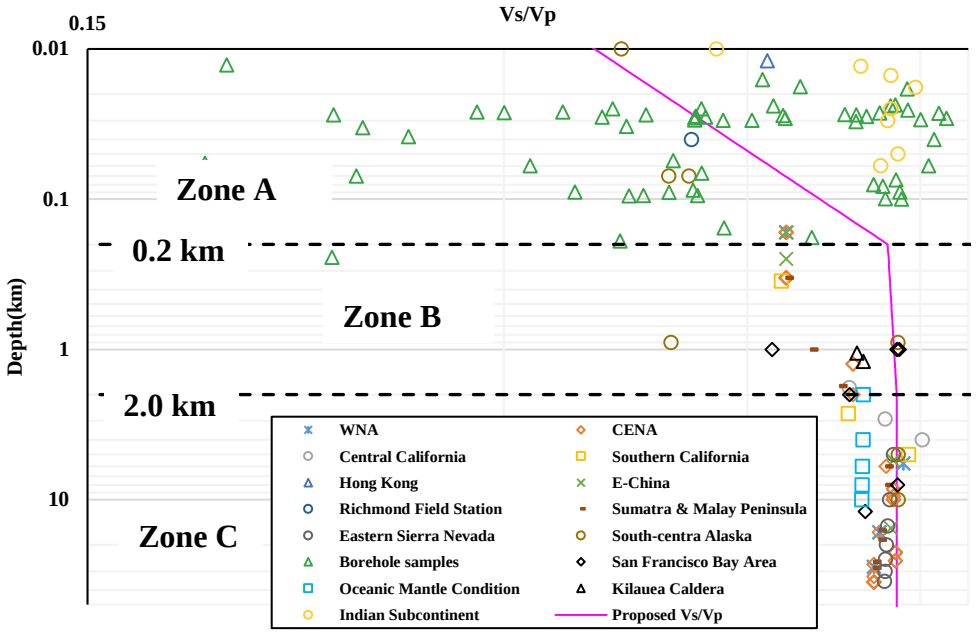

Figure 2. Proposed V_S/V_P model

$$0.5684*(Z/0.2)^{0.163} \quad Z \leq 0.2 \tag{3a}$$

$$0.577*(Z/2)^{0.00652} \quad 0.2 < Z \leq 2 \tag{3b}$$

$$0.577 \quad Z > 2 \tag{3c}$$

Five representative V_S-V_P relationship equations obtained from various data records global around are summarized in Table 2 for comparison purpose. Among these equations, **Cea85** (Castagna, et al. 1985), **Han86** (Han 1986), **B05** (Brocher 2005), **CLT05** (Chandler, et al. 2005) are all for general use global around, while **Pea15** (Parvizi, et al. 2015) is specific for Gachsaran regions, in Iran (Middle East). These models are adopted to verify the validation of the proposed V_S-V_P relationship. The result can be found in **Figure 3**, alongside the same dataset shown in **Figure 2**.

Table 2. V_S-V_P relationship equations used for uncertainty analysis

Equations	Citations
$V_S = 0.862V_P - 1.172$	Castagna, et al. (1985)
$V_S = 0.794V_P - 0.787$	Han (1986)
$V_S = 0.7858 - 1.2344V_P + 0.7949V_P^2 - 0.1238V_P^3 + 0.0064V_P^4$	Brocher (2005)
$\frac{V_S}{V_P} = 0.58\left(\frac{Z}{4}\right)^{\frac{1}{12}}, \ Z \leq 4;$ $\frac{V_S}{V_P} = 0.58, \ Z > 4.$	Chandler, et al. (2005)
$V_S = 4.226 - 7.465/V_P$	Parvizi, et al. (2015)

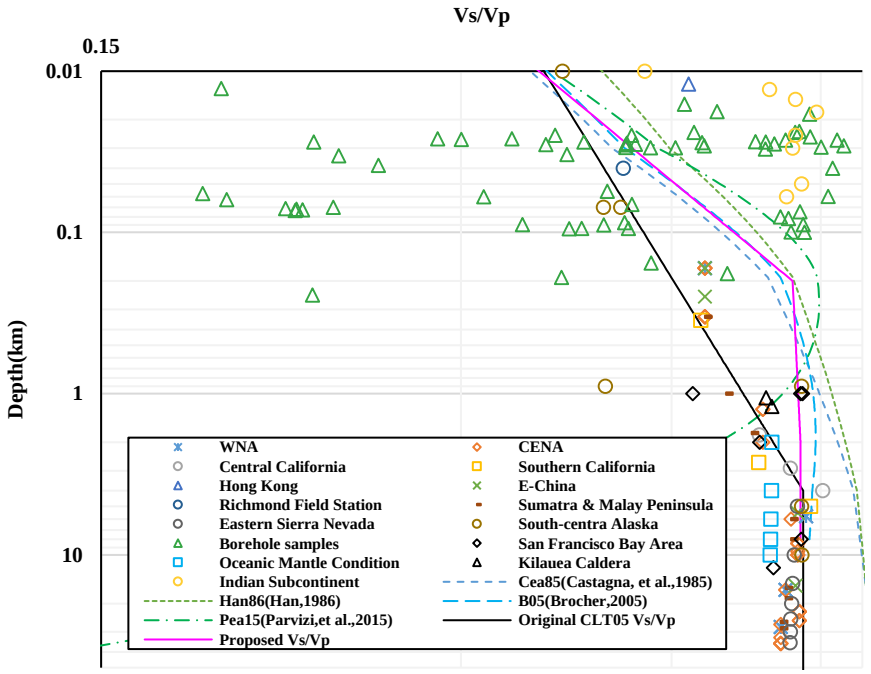

Figure 3. Comparison analysis of proposed V_S/V_P with 5 selected V_S-V_P relationships, alongside with recording data.

Figure 3 shows that, except **CLT05** model and **Pea15** model, other models can obtain similar estimates of V_S/V_P. The proposed V_S/V_P in this study matches **B05** model very well. This can be an indication that the proposed V_S/V_P is reasonably accurate.

2.3 Shear-wave velocity profile modelling

Based on the results obtained from section 3.1 and 3.2, the shear-wave velocity profile can be modelled by combining the compressional wave velocity profile and V_S/V_P model. To assist for understanding the shear-wave velocity profile modelling process, **Figure 4** is adopted for better illustration.

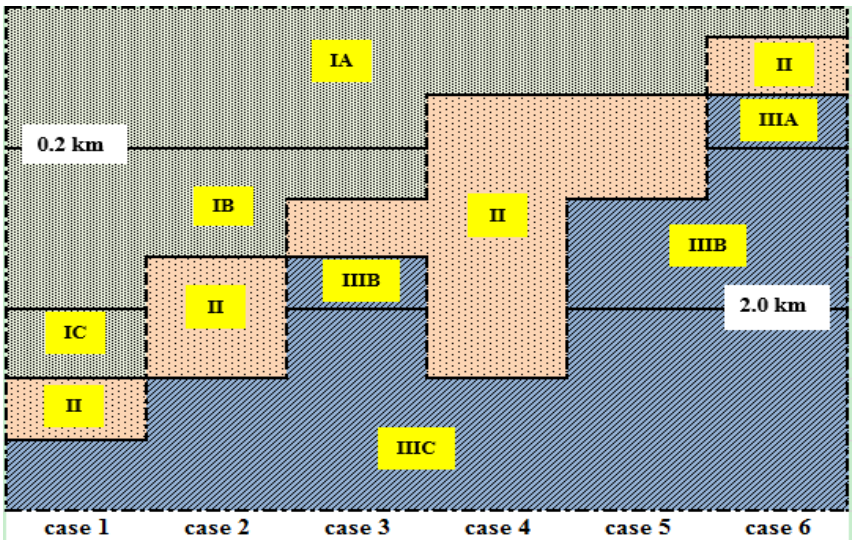

Figure 4. Illustration of shear-wave velocity profile modelling. Seven different zones are defined for V_S profile modelling.

The zone-by-zone modelling process is presented in following sections.

The detailed functional forms for the six frequently encountered cases, and their corresponding zones, are summarized in **Table 3.**

Table 3. The functional forms of SWV profile model

Depth range (km)	Vs (km/s)	Zone
Case 1 ($Z_S \geq 2$)		
$0 < Z \leq 0.2$	$V_{S0.03}*(Z/0.03)^{0.3297}$	IA
$0.2 < Z \leq 2$	$V_{S0.2}*(Z/0.2)^{0.1732}$	IB
$2 < Z \leq Z_S$	$V_{S2}*(Z/2)^{0.1667}$	IC
$Z_S < Z \leq Z_C$	$V_{SZc}*(Z/Z_C)^{n}$	II
$Z_C < Z$	$V_{S8}*(Z/8)^{0.0833}$	IIIC
Case 2 ($0.2 < Z_S < 2 \leq Z_C$)		
$Z \leq 0.2$	$V_{S0.03}*(Z/0.03)^{0.3297}$	IA
$0.2 < Z \leq Z_S$	$V_{S0.2}*(Z/0.2)^{0.1732}$	IB
$Z_S < Z \leq Z_C$	$V_{SZc}*(Z/Z_C)^{n}$	II
$Z_C < Z$	$V_{S8}*(Z/8)^{0.0833}$	IIIC
Case 3 ($0.2 < Z_S < Z_C \leq 2$)		
$0 < Z \leq 0.2$	$V_{S0.03}*(Z/0.03)^{0.3297}$	IA
$0.2 < Z \leq Z_S$	$V_{S0.2}*(Z/0.2)^{0.1732}$	IB
$Z_S < Z \leq Z_C$	$V_{SZc}*(Z/Z_C)^{n}$	II
$Z_C < Z \leq 2$	$V_{S2}*(Z/2)^{0.0899}$	IIIB
$2 < Z$	$V_{S8}*(Z/8)^{0.0833}$	IIIC
Case 4 ($Z_S < 0.2 < 2 \leq Z_C$)		
$0 < Z \leq Z_S$	$V_{S0.03}*(Z/0.03)^{0.3297}$	IA
$Z_S < Z \leq Z_C$	$V_{SZc}*(Z/Z_C)^{n}$	II
$Z_C < Z$	$V_{S8}*(Z/8)^{0.0833}$	IIIC
Case 5 ($Z_S < 0.2 < Z_C \leq 2$)		
$Z \leq Z_S$	$V_{S0.03}*(Z/0.03)^{0.3297}$	IA
$Z_S < Z \leq Z_C$	$V_{SZc}*(Z/Z_C)^{n}$	II
$Z_C < Z \leq 2$	$V_{S2}*(Z/2)^{0.0899}$	IIIB
$2 < Z$	$V_{S8}*(Z/8)^{0.0833}$	IIIC
Case 6 ($Z_C \leq 0.2$)		
$0 < Z \leq Z_S$	$V_{S0.03}*(Z/0.03)^{0.3297}$	IA
$Z_S < Z \leq Z_C$	$V_{SZc}*(Z/Z_C)^{n}$	II
$Z_C < Z \leq 0.2$	$V_{S0.2}*(Z/0.2)^{0.2463}$	IIIA
$0.2 < Z \leq 2$	$V_{S2}*(Z/2)^{0.0899}$	IIIB
$2 < Z$	$V_{S8}*(Z/8)^{0.0833}$	IIIC

It is important to note that, in all cases, Zone II is a transition zone that is used to connect the upper zone and lower zone. Thus, the functional form is the same, except the value of exponent "*n*". In all cases, *n* is expressed by equation (4):

$$n = \frac{\log(V_{SZc}/V_{SZs})}{\log(Zc/Zs)} \tag{4}$$

where V_{SZc} and V_{SZs} are the shear-wave velocity value at the depth of Z_C and Z_S km, and their values are changing for all cases, thus the value of *n* changes case by case.

The estimation of Z_C and Z_S values are essential for constructing reasonable V_S profiles. The detailed four approaches for obtaining Z_C and Z_S values can be found from the descriptions in section 5 in Chandler, et al. (2005).

The models described above are all for non-glaciated crustal conditions. However, in many regions, they are underlain by harder rock, resulting from extensively glaciation. The universally applicable V_S profile model, which incorporates the depth of glaciated layer (Zg), is described by equation (5a) to (5g), in a zone-by-zone format.

i) Zone IA

$$V_S = V_{S0.03}*(Z + Zg / 0.03 + Zg)^{0.3297}, \quad Z+Zg \leq Z_S \tag{5a}$$

ii) Zone IB

$$V_S = V_{S0.2\text{-}Zg}*(Z + Zg / 0.2)^{0.1732}, \; 0.2 < Z + Zg \leq Z_S \tag{5b}$$

iii) Zone IC

$$V_S = V_{S2\text{-}Zg}*(Z + Zg / 2)^{0.1667}, \quad 2 < Z + Zg \leq Z_S \tag{5c}$$

iv) Zone II

$$V_S = V_{SZc}*(Z + Zg / Z_C + Zg)^{n}, \quad n = \frac{\log(V_{SZc}/V_{SZs})}{\log(Zc/Zs)} \tag{5d}$$

v) Zone IIIA

$$V_S = V_{S0.2\text{-}Zg}*(Z + Zg/ 0.2)^{0.2463}, \; Z_C < Z + Zg \leq 0.2 \tag{5e}$$

vi) Zone IIIB

$$V_S = V_{S2\text{-}Zg}*(Z + Zg/ 2)^{0.0899}, \quad 0.2 < Z + Zg \leq 2 \tag{5f}$$

vii) Zone IIIC

$$V_S = V_{S8}*(Z+Zg/ 8+Zg)^{0.0833}, \; Z+Zg > Z_C \tag{5g}$$

In this study, the depth of top glaciation layer Zg is assumed to fall within the lower sedimentary layer (Zone II), and it needs to be identified before applying equation (5). In most cases, Zg value cannot be determined directly, even CRUST1.0 does not contain much information about Zg. A simplified methodology of determining Zg will be put forward in section 4.

References

Abercrombie, R. E. (1997). "Near-surface Attenuation and Site Effects from Comparison of Surface and Deep Borehole Recordings " Bull. Seismol. Soc. Am. **87**: 731-744.

Allen, T. I. (2012). Stochastic ground-motion prediction equations for southeastern Australian earthquakes using updated source and attenuation parameters. G. Australia. Canberra. **2012/69**.

Archuleta, R. J. (1982). "Analysis of near source static and dynamic measurements from the 1979 Imperial Valley earthquake." Bull. Seismol. Soc. Am. **72**: 1927-1956.

Atkinson, G. M. (2004). "Empirical Atteunation of Ground Motion Spectral Amplitudes in Southeastern Canada and the Northeastern United States." Bull. Seismol. Soc. Am. **94**: 1079-1095.

Atkinson, G. M. (2008). "Ground-Motion Prediction Equations for Eastern North America from a Referenced Empirical Approach: Implications for Epistemic Uncertainty." Bull. Seismol. Soc. Am. **98**(3): 1304-1318.

Atkinson, G. M. and D. M. Boore (1995). "Ground-Motion Relations for Eastern North America." Bull. Seismol. Soc. Am. **85**(1): 17-30.

Atkinson, G. M. and D. M. Boore (2006). "Earthquake Ground-Motion Prediction Equations for Eastern North America." Bull. Seismol. Soc. Am. **96**(6): 2181-2205.

Atkinson, G. M. and D. M. Boore (2014). "The Attenuation of Fourier Amplitudes for Rock Sites in Eastern North America." Bull. Seismol. Soc. Am. **104**(1): 513-528.

Bhowmick, S. (2017). "Role of Vp/Vs and Poisson's Ratio in the Assessment of Foundation(s) for Important Civil Structure(s)." Geotech Geol Eng **35**: 527-534.

Boore, D. M. (2003b). P- and S- Velocities from Surface-to-Borehole Logging. U.S, USGS**:** 14.

Boore, D. M. and W. B. Joyner (1997). "Site Amplifications for Generic Rock Sites." Bull. Seismol. Soc. Am. **87**(2): 327-341.

Brocher, T. M. (2005). "Empirical relations between elastic wavespeeds and density in the Earth's crust." Bull. Seismol. Soc. Am. **95**(6): 2081-2092.

Chandler, A. M., et al. (2005). "Shear wave velocity modelling in crustal rock for seismic hazard analysis." Soil Dynamics and Earthquake Engineering **25**: 167-185.

Fliedner, M. M. and S. Klemperer (2000). "Three-dimensional seismic model of the Sierra Nevada arc California and its implications for crustal and upper mantle composition." JOURNAL OF GEOPHYSICAL RESEARCH, **105**(B5): 10899-10921.

Han, D. H. (1986). Effects of porosity and clay content on acoustic properties of sandstones and unconsolidated sediments. Department of Geophysics. Stanford, USA., Stanford University. **Ph.D.**

Tam, K. W. (2002). Anisotropy in seismic wave velocity in jointed rocks in Hong Kong, The University of Hong Kong. **MPhil**.

Yenier, E. and G. M. Atkinson (2015). "Regionally Adjustable Generic Ground-Motion Prediction Equation Based on Equivalent Point-Source Simulations: Application to Central and Eastern North America." Bull. Seismol. Soc. Am. **105**(4): 1989-2009.

Appendix

Table I. Geological location of sampling points for the study region

No.	Name	Latitude	Longitude
Western Australia (WA)			
1	Minilya	-23.8225	114.6094
2	Carnarvon	-24.8466	113.6646
3	Geraldton	-28.7965	114.6204
4	Cervantes	-30.5055	115.0708
5	Perth	-31.9335	115.8618
6	Bunbury	-33.2846	115.6421
7	Busselton	-33.6512	115.3564
8	Albany	-35.012	117.8613
9	Esperance	-33.8339	121.9043
South-eastern Australia (SEA)			
1	Greater Taree	-31.8236	152.2946
2	Newcastle	-32.9322	151.7522
3	Central Coast	-33.3695	151.4438
4	Sydney	-33.8958	151.2039
5	Wollongong	-34.4353	150.8849
6	Canberra	-35.3335	149.1241
7	Lake Entrance	-37.8488	148.0023
8	Melbourne	-37.7938	144.9688
9	Geelong	-38.1453	144.3540
10	Warnambool	-38.3717	142.4916
11	Mount Grambier	-37.8305	140.7806
12	Tilley Swamp	-36.3417	139.8449
13	Adelaide	-34.9442	138.5960
Western North America (WNA)			
1	Wilderville	42.391	-123.442
2	Fruitland	40.36328	-123.772
3	Ingram	38.92522	-123.157
4	San Francisco	37.78808	-122.388
5	Johnson Canyon	36.54494	-121.421
6	Creston	35.5501	-120.52
7	Los Angeles	34.07086	-118.257
8	San Diego	32.73184	-117.18
Glaciated WNA			
1	Neechantz Peak	51.4261	-126.914
2	Bonanza Peak	50.28933	-126.826
3	Mt Tinniswood	50.31609	-123.851
4	Port Alberni	49.1817	-124.937
5	Van Zandt	48.79126	-122.181
6	Seattle	47.60616	-122.322
7	Portland	45.50634	-122.695
Eastern North America (ENA)			
1	New Durham	43.45291	-71.1914
2	Belchertown	42.26266	-72.3776
3	New York	40.67857	-73.9407
4	Philadelphia	39.97712	-75.1904
5	Washington	38.92522	-77.0361
6	Richmond	37.61423	-77.3877

7	Rocky Mount	35.89364	-77.7389
8	Florence	34.19817	-79.4971
9	Milbury	32.91648	-81.5186
10	Jacksonville	30.34561	-81.6888
	Glaciated ENA		
1	Port-Cartier	50.48547	-67.2363
2	Micoua	49.78126	-68.7305
3	Murdochville	48.74894	-65.4785
4	Glen Emma	48.07807	-67.4561
5	Doaktown	46.52863	-66.0938
6	Ashland	46.67959	-68.4668
7	Seboeis Public Reserved Lands	45.52174	-68.9941
8	East Milton	44.4965	-70.6201
	South-eastern China (SEC)		
1	Nantong	32.0087	120.9155
2	Shanghai	31.24098	121.4539
3	Hangzhou	30.29701	120.1575
4	Taizhou	28.67131	121.4209
5	Wenzhou	27.9944	120.6958
6	Ningde	26.68672	119.5532
7	Fuzhou	26.08638	119.3005
8	Quanzhou	24.88643	118.6853
9	Xiamen	24.48714	118.092
10	Shantou	23.36242	116.6748
11	Shanwei	22.79137	115.3729
12	Shenzhen	22.543	114.0601
13	Hong Kong	22.42626	114.115
14	Yangjiang	21.86149	111.9727
15	Maoming	21.66253	110.918